

Kinetic Modeling of the Fischer-Tropsch Reactions and Modeling Steady State Heterogeneous Reactor

M. Ahmadi Marvast, M. Sohrabi, H. Ganji

Abstract—The rate of production of main products of the Fischer-Tropsch reactions over Fe/HZSM5 bifunctional catalyst in a fixed bed reactor is investigated at a broad range of temperature, pressure, space velocity, H₂/CO feed molar ratio and CO₂, CH₄ and water flow rates. Model discrimination and parameter estimation were performed according to the integral method of kinetic analysis. Due to lack of mechanism development for Fischer – Tropsch Synthesis on bifunctional catalysts, 26 different models were tested and the best model is selected. Comprehensive one and two dimensional heterogeneous reactor models are developed to simulate the performance of fixed-bed Fischer – Tropsch reactors. To reduce computational time for optimization purposes, an Artificial Feed Forward Neural Network (AFFNN) has been used to describe intra particle mass and heat transfer diffusion in the catalyst pellet. It is seen that products' reaction rates have direct relation with H₂ partial pressure and reverse relation with CO partial pressure. The results show that the hybrid model has good agreement with rigorous mechanistic model, favoring that the hybrid model is about 25-30 times faster.

Keywords—Fischer-Tropsch, Heterogeneous modeling, Kinetic study.

I. INTRODUCTION

IN Fischer-Tropsch (FT) process, the synthesis gas, i. e. a mixture of predominantly CO and H₂, obtained from coal, biomass or natural gas is converted to a multicomponent mixture of hydrocarbons. Currently, a promising field in energy utilization is the conversion of natural gas to environmentally clean fuels, specialty chemicals and waxes.

Fuels produced from the FT process are of high quality due to a very low aromaticity and absence of sulfur. However, due to the limitation of Schulz – Flory distribution [1], the yield of the hydrocarbons within the range of those presented in gasoline is low. At the same time, the octane number of FT gasoline is lower than that of the gasoline obtained from the crude oil processing, as the FT gasoline is mainly consisted of n-paraffin. To improve the yield and quality of the gasoline from the FT synthesis, the bifunctional catalysts have received

extensive attention in the recent years [2], [3].

Various types of reactors (including fixed bed, fluidized – bed and slurry) have been considered during the FTS process development. The fixed – bed Fischer Tropsch process, being one of the most competing reactor technologies, occupies a special position in FTS industrial practices, as persuasively exemplified by the large scale commercial operations of Sasol [4] and Shell [5].

The new GTL process based on one staged fixed bed FT synthesis was developed in the Research Institute of Petroleum Industry (RIPI) to produce high octane, low sulfur Gasoline [6]. In this process the modified Bifunctional Fe – HZSM5 catalyst has been used [3], [7], [8]. Such a process removes the need for the cumbersome upgrading unit for GTL plants.

To achieve an optimum performance for the complete process, the catalyst and the reactor should be comprehensively optimized. Evidently, due to the complexity of FTS reaction system, a proper kinetic study, from which the selectivity information can be determined in a quantitative fashion, has to be presented.

The kinetics of the Fischer–Tropsch synthesis have been studied extensively to describe the reaction rate using a power law rate equation or an equation based on certain mechanistic assumptions [9-12]. Literature reviews indicate a few reports on the kinetic study on bifunctional catalysts and also product's reaction rates determination.

It seems that the effects of bifunctional catalysts on the selectivity of products and performance of the reactor and mass and heat transfer in 2D have not been yet considered.

In order to develop comprehensive two-dimensional heterogeneous modeling of FTS reactor, we studied the one and two dimensional pseudo homogeneous steady state behavior of fixed bed FT catalytic reactor over bifunctional catalyst [13].

As a continuing parts of these preliminary efforts, in the present study, the one and two-dimensional heterogeneous models for Fischer – Tropsch fixed bed reactors have been developed. The proposed models have been validated by the experimental data.

In order to calculate the global reaction rates at each point of the reactor, the mass and energy balances inside the pellet must be performed. This procedure may be time consuming. In this regard, a hybrid model included mechanistic pseudo homogeneous model for the gas phase and AFFNN (Artificial Feed Forward Neural Network) for solid phase has been

M. Ahmadi Marvast is with the Engineering Development Division, Research Institute of Petroleum Industry, Tehran, Iran (phone: +98-21-44739792; fax: +98-21-44739713; e-mail: ahmadim@ripi.ir).

M. Sohrabi, is with the Department of Chemical Engineering, Amir Kabir University, Tehran, Iran (e-mail: sohrabi@aut.ac.ir).

H.Ganji is with the Engineering Development Division, Research Institute of Petroleum Industry, Tehran, Iran (phone: +98-21-48252120; fax: +98-21-44739713; e-mail: ganjih@ripi.ir).

developed. Over 2000 data points that have been obtained from mechanistic one dimensional heterogeneous model results have been used to train AFFNN.

In the present study, the basic kinetic features of functioning of this type of catalyst for purpose of further development and optimization of the reactor model were studied.

II. ARTIFICIAL NEURAL NETWORKS

Artificial neural networks (NN) consist of a number of simple interconnected processing units, also called neurons, which are analogous to the biological neurons. An NN is an oriented graph in which the neurons represent a set of processing units and the arches (or connections) represent the information flow channels. Each connection between two neurons has an associated value called weight (w_{ij}) which specifies the strength of the connection from unit j to unit i . The schematic diagram of a single neuron is shown in Fig. 1. The input to each neuron consists of an N -dimensional vector X and a single bias (threshold) b .

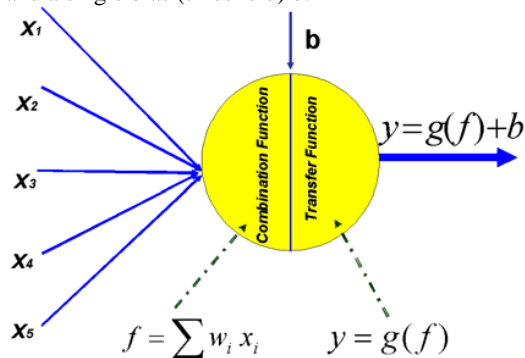


Fig. 1 Schematic diagram of a single neuron.

One of the most well known structures of neuronal networks for supervised learning is the multi-layer perceptron, which is generally used for classification and prediction problems [14]. In the multi-layer perceptron, neurons are grouped into layers. An example of a layered network is shown in Fig. 2. In this network an input layer, two hidden layers and an output layer can be seen. The output of the j th hidden unit is obtained by first forming a weighted linear combination of the d input values, giving:

$$a_j = \sum_{i=0}^d w_{ji} x_i \quad (1)$$

Here, w_{ji} denotes a weight going from input i to hidden unit j and x_i denotes the input i of the neuron. Then, using an activation function g , final output of neurons are obtained:

$$z_j = g(a_j) \quad (2)$$

In this paper, we have used the most common type of ANN (Artificial Neural Network) with multiple layers and supervised learning called Feed Forward (AFFNN) or back propagation network [15].

Sigmoidal activation functions are widely applied in NNs.

In this work, logistic and tangential sigmoidal functions have been employed for the hidden units.

$$g(a_j) = \frac{1}{1 + e^{-a_j}} \quad (\text{logistic sigmoidal function})$$

$$g(a_j) = \frac{e^{a_j} - e^{-a_j}}{e^{a_j} + e^{-a_j}} \quad (\text{tangential sigmoidal function})$$

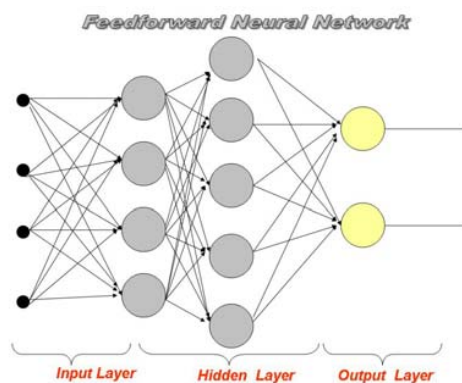


Fig. 2 Structure of an AFFNN.

Two important features of neural networks are the ability of supplying fast answers to a problem and the capability of generalizing their answers, providing acceptable results for unknown samples. In this way, they need to learn about the problem under study and this learning is commonly named training process. This process usually starts with random values for the weights of the NN. Then, NN are supplied with a set of samples belonging to the problem domain and they establish mathematical correlation between the samples [20], modifying the values of their weights.

Two main modelling strategies employing neural networks may be distinguished: the first one called 'the black-box approach', when the entire process is represented with the appropriate neural net, and 'the hybrid approach', which is a combination of both; traditional modelling of the process and a neural network representing the less known phenomena of the process. In the former case a generalization of the obtained results to other systems, e.g. differing in size or operating conditions is hardly possible, while the latter approach gives an exciting opportunity for knowledge generalization. This hybrid approach, since its introduction by Psychogios and Ungar [16], has been found to be smart and efficient to model complex reacting systems with unknown kinetics [16] and heterogeneous modeling [17].

III. EXPERIMENTAL

For kinetic study on the RPI's catalyst, 53 different experiments were performed in an isothermal integral fixed bed reactor and in no diffusion limitation conditions. Based on the design of experiments, concentrations of CO, H₂, CH₄, CO₂ and H₂O and temperature, pressure and GHSV at the inlet of reactor has been changed and the reactor output was analyzed. The primary products' rate of production was tested

with different kinetic models and best model and parameters were developed.

A. Experimental system

The experimental setup was designed and constructed based on fixed bed reactor (Fig. 3). It has 4 main sections including:

1) Feed section

Flow rates of H_2 (99.999%), CO (99.5%), N_2 (99.999%), CO_2 (99.95%), CH_4 (99.99%) were controlled through MFCs (Mass Flow Controller) and then entered to a Gas Mixing Chamber for better mixing. Water was mixed as vapor with the gases and the mixture entered the reactor section.

2) Reactor section

There was a 2 parts reactor (Fig. 4). The first part was a stainless steel tube with internal diameter of 0.635 cm and length of 40 cm. This part was used for preheating the feed that is passed to the reaction section. In the second part, the catalyst was loaded in a stainless steel tube with internal diameter of 1.12 cm and length of 30 cm.

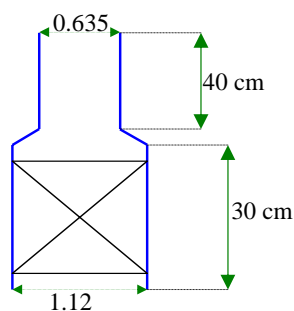


Fig. 4. The reactor schematic diagram

Fischer-Tropsch products consist of gaseous, aqueous and oil phases. The corresponding chromatography analysis conditions for determining the composition of the tail gas, oil and water phases are summarized in Table 1. The products in the gaseous and oily phases are identified by spiking a sample with standard compounds.

TABLE I CHROMATOGRAPHY OPERATING CONDITIONS FOR PRODUCT ANALYSIS

GC mode	Stationary phase	Column temperature (K)	Detector	Carrier (ml/min)	Sample size	Components
4CPTF	Propack Q	Room temperature	TCD	Ar (25)	0.6 ml	CO_2 , CH_4 , C_2H_4
4CPTF	Molecular sieve	Room temperature	TCD	Ar (25)	0.6 ml	H_2 , CH_4 , CO
CP-3800	Chromosorb	340-400	TCD	He (15)	0.6 ml	C_1 - C_3 hydrocarbons
CP-3800	Fused Capillary	450-580	FID	He (15)	0.4 μ l	C_3 - C_{22} hydrocarbons

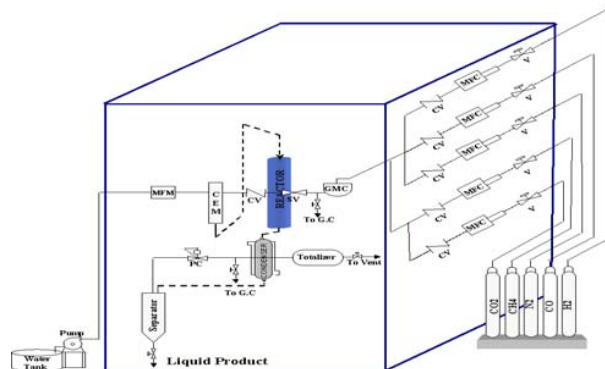


Fig. 3. Experimental setup. V: Valve, MFC: Mass Flow Controller, CV: Check Valve, SV: Safety Valve, MFM: liquid Mass Flow Meter, CEM: Control, Evaporation, Mixture for liquid, PC: Pressure Controller

3) Separation section

The liquid product was collected in an ice trap (Ca. 273.2 °C) at system pressure. After system pressure was released through a back pressure regulator, the tail gas leaving the ice trap is measured by a wet gas flow meter.

4) Product analysis

The product stream was split into two parts: gas phase and liquid phase. The liquid products collected in the ice trap were then separated into the water and oil phases. Hence, the

B. Experimental procedure

Experiments were carried out by using catalyst particles with a diameter between 50-60 ASTM mesh. In this range of catalyst diameter, no internal diffusion was detected. 1.5 g of catalyst was diluted at a 1:8 ratio (catalyst to inert, v/v) with quartz sand of the same mesh size range. To match the conditions of the exclusion of external diffusion limitation, the kinetic experiments were performed by using high space velocities. The space velocities of 3000 – 6000 h^{-1} were adopted in our work. For confirming isothermal conditions, the maximum temperature difference between reactor center and surface along the bed was reported as 1 °C. The maximum temperature difference of 0.5 °C is reported along the reactor bed.

By optimal design method, a total of 53 sets of experimental data were obtained for detailed kinetic study. The reactor and catalyst characteristics are shown in Table 2.

The main components for the rate of production study was selected as: CH_4 , CO_2 , C_2H_4 , C_2H_6 , C_3H_8 , $n-C_4$, $i-C_4$ (as the main products of gas phase), H_2O (as one of the main products) and C_5^+ (as the oily product plus gas phase products of $i-C_5$, $n-C_5$, $i-C_6$, $n-C_6$, Benzene and Toluene).

TABLE II CATALYST AND REACTOR SPECIFICATION

Reactor ID (cm)	1.12	Bed porosity	0.4
Bed length (cm)	18	Bed density (kg/m ³)	84.65

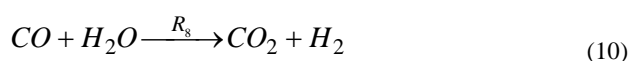
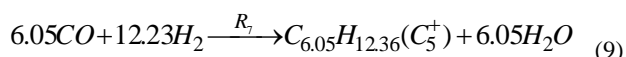
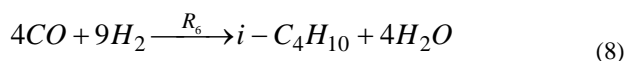
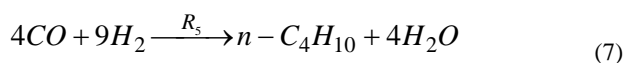
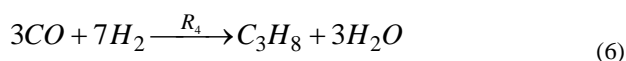
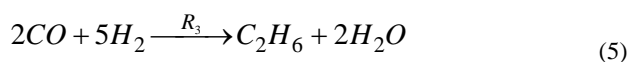
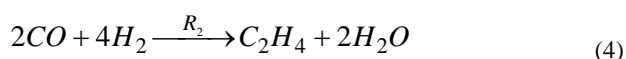
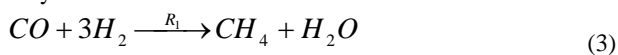
IV. MODEL DISCRIMINATION AND PARAMETER ESTIMATION

As there has not been developed any mechanism for Fischer – Tropsch reactions on bifunctional Fe-HZSM5 catalyst, the major kinetic models developed for iron catalyst has been tested. To find the best model for bifunctional catalyst, some extra models derived from the main kinetic models of the iron catalyst. The total number of 26 kinetic models (Table 3) has been optimized based on the experimental results.

For parameter estimation of each model, the kinetic parameters were optimized to satisfy the experimental result by using one dimensional isothermal modeling of the reactor. The flow chart of the parameter estimation program is shown in Fig 5.

A. One dimensional isothermal modeling of the reactor

The reactions for producing main components in the kinetic study are as follow:



In this model, the following assumptions have been made:

1. The reactor is taken to be under steady state conditions.
2. The model is pseudo homogeneous (i.e. there is no concentration and temperature gradients within the catalyst pellet)
3. There is no radial concentration and temperature gradients in the reactor (i. e. one dimensional model in axial direction).
4. There is no gas radial velocity in the reactor.

5. The radial and axial dispersion has been ignored.

6. There is no temperature gradient across the bed (isothermal reactor).

The mass and energy equations for the bulk gas phase (pseudo homogeneous model) can be written as follows:

$$-\frac{d(u_s C_i)}{dl} = \rho_p R_i \quad i = 1, 2, \dots, NC \quad (11)$$

$$\frac{d(u_s \rho_g C_p T)}{dl} = \rho_p \sum_{j=1}^{NR} (-\Delta H)_j R_j + \frac{4U}{2R} (T_w - T) \quad j = 1, 2, \dots, NR \quad (12)$$

For the pressure drop, the following equation is used (Ergun Equation):

$$\frac{dP}{dl} = - \left(1.75 + 150 \left(\frac{1 - \varepsilon_b}{d_p G / \mu} \right) \right) \frac{G^2}{1.01325 \times 10^6 d_p \rho_g} \left(\frac{1 - \varepsilon_b}{\varepsilon_b^3} \right) \quad (13)$$

The initial conditions for the bulk phase are given as:

$$l=0, C_i = C_{i,0}; P = P_{in}; T = T_{in} \quad (14)$$

B. Results and discussion

For parameter estimation of each model, the following criteria had to be satisfied:

$$\theta = \sum_j \sum_i \left((C_{ij,out})_{exp} - (C_{ij,out})_{cal} \right)^2 < Tol. \quad (15)$$

In which i and j denote to component and experiment numbers respectively; C, component concentration; exp. and cal., experimental and calculated results. Tolerance (Tol.) of 10^{-10} was being used.

The results of parameter estimation for different models are being shown in Table 4.

By these results, the model discrimination is being performed. Kinetic model No. 12 gives the least goal function (θ). The selected model and its parameters are shown in Table 5.

The model discrimination results show that:

Deleting of Water partial pressure from kinetic model enhances the model results to the experimental one (comparison between results of models No. 1 & 3).

CO₂ partial pressure does not have an important effect on rate of production of the main products (comparison between results of models No. 14, 16, 17 & 18).

Methane partial pressure is not being an important factor in rate of production of the main products (comparison between results of models No. 14, 24, 25 & 26).

C₅⁺ partial pressure does not have an important effect on rate of production (comparison between results of models No. 14 & 19).

TABLE III KINETIC MODELS USED FOR MODEL DISCRIMINATION

No.	Reference	Kinetic Model (R _i)	No.	Reference	Kinetic Model (R _i)
1	8	$K_1 \exp\left(\frac{-E_1}{RT}\right) \frac{P_{H_2}^2 P_{CO}}{P_{H_2O} + K_2 P_{H_2} P_{CO}}$	14	This research	$K_1 \exp\left(\frac{-E_1}{RT}\right) \frac{P_{H_2}^2}{P_{CO}}$
2	This research	$K_1 \exp\left(\frac{-E_1}{RT}\right) \frac{P_{H_2}^2 P_{CO}}{P_{H_2O}^2 + K_2 P_{H_2} P_{CO}}$	15	This research	$K_1 \exp\left(\frac{-E_1}{RT}\right) \frac{P_{H_2}^2}{P_{CO}^2}$
3	4	$K_1 \exp\left(\frac{-E_1}{RT}\right) P_{H_2}$	16	This research	$K_1 \exp\left(\frac{-E_1}{RT}\right) \frac{P_{H_2}^2}{K_2 P_{CO} + P_{CO_2}}$
4	This research	$K_1 \exp\left(\frac{-E_1}{RT}\right) \frac{P_{H_2}^2 P_{CO}}{10 P_{H_2O} + K_2 P_{H_2} P_{CO}}$	17	This research	$K_1 \exp\left(\frac{-E_1}{RT}\right) \frac{P_{H_2}^2}{K_2 P_{CO} + P_{CO_2}^2}$
5	8	$K_1 \exp\left(\frac{-E_1}{RT}\right) \frac{P_{H_2} P_{CO}}{P_{H_2O} + K_2 P_{CO}}$	18	This research	$K_1 \exp\left(\frac{-E_1}{RT}\right) \frac{P_{H_2}^2}{K_2 P_{CO} + 10 P_{CO_2}^2}$
6	This research	$K_1 \exp\left(\frac{-E_1}{RT}\right) P_{H_2}^2$	19	This research	$K_1 \exp\left(\frac{-E_1}{RT}\right) \frac{P_{H_2}^2}{K_2 P_{CO} + P_{C_s^+}}$
7	This research	$K_1 \exp\left(\frac{-E_1}{RT}\right) P_{H_2}^{K_2}$	20	This research	$K_1 \exp\left(\frac{-E_1}{RT}\right) P_{CO}$
8	This research	$K_1 \exp\left(\frac{-E_1}{RT}\right) P_{H_2}^{K_2} P_{CO}$	21	This research	$K_1 \exp\left(\frac{-E_1}{RT}\right) \frac{P_{CO}}{P_{H_2}}$
9	This research	$K_1 \exp\left(\frac{-E_1}{RT}\right) \frac{P_{H_2}^{K_2}}{P_{CO}}$	22	This research	$K_1 \exp\left(\frac{-E_1}{RT}\right) P_{CO}^2$
10	This research	$K_1 \exp\left(\frac{-E_1}{RT}\right) P_{H_2}^{K_2} P_{CO}^2$	23	18	$K_1 \exp\left(\frac{-E_1}{RT}\right) P_{H_2}^{K_2} P_{CO}^{K_3}$
11	This research	$K_1 \exp\left(\frac{-E_1}{RT}\right) P_{H_2}^2 P_{CO}^2$	24	This research	$K_1 \exp\left(\frac{-E_1}{RT}\right) \frac{P_{H_2}^2}{K_2 P_{CO} + P_{CH_4}}$
12	This research	$K_1 \exp\left(\frac{-E_1}{RT}\right) \frac{P_{H_2}^2}{P_{CO}}$	25	This research	$K_1 \exp\left(\frac{-E_1}{RT}\right) \frac{P_{H_2}^2}{K_2 P_{CO} + P_{CH_4}^2}$
13	This research	$K_1 \exp\left(\frac{-E_1}{RT}\right) \frac{P_{H_2}^2}{P_{CO}^2}$	26	This research	$K_1 \exp\left(\frac{-E_1}{RT}\right) \frac{P_{H_2}^2}{K_2 P_{CO} + 10 P_{CH_4}}$

C. Neural Network approximation

As mechanistic two dimensional heterogeneous modeling of FT industrial reactor is so complicated and time consuming, we are seeking here to obtain a simple expression (by neural network) for components' effectiveness factor as a function of partial pressures and temperature in the gas phase. This neural network expression must reproduce the complex behavior of

effectiveness factors. Figure 6 shows this strategy. The reactor is simulated in a range of operating conditions by one dimensional heterogeneous model; in which simultaneous gas and solid phases equation are solved. To produce a reliable data for the training of neural network, effectiveness factors along the reactor is being calculated by a series of results

obtained from different operating conditions. Operating conditions is being changed in the limits as shown in table 6.

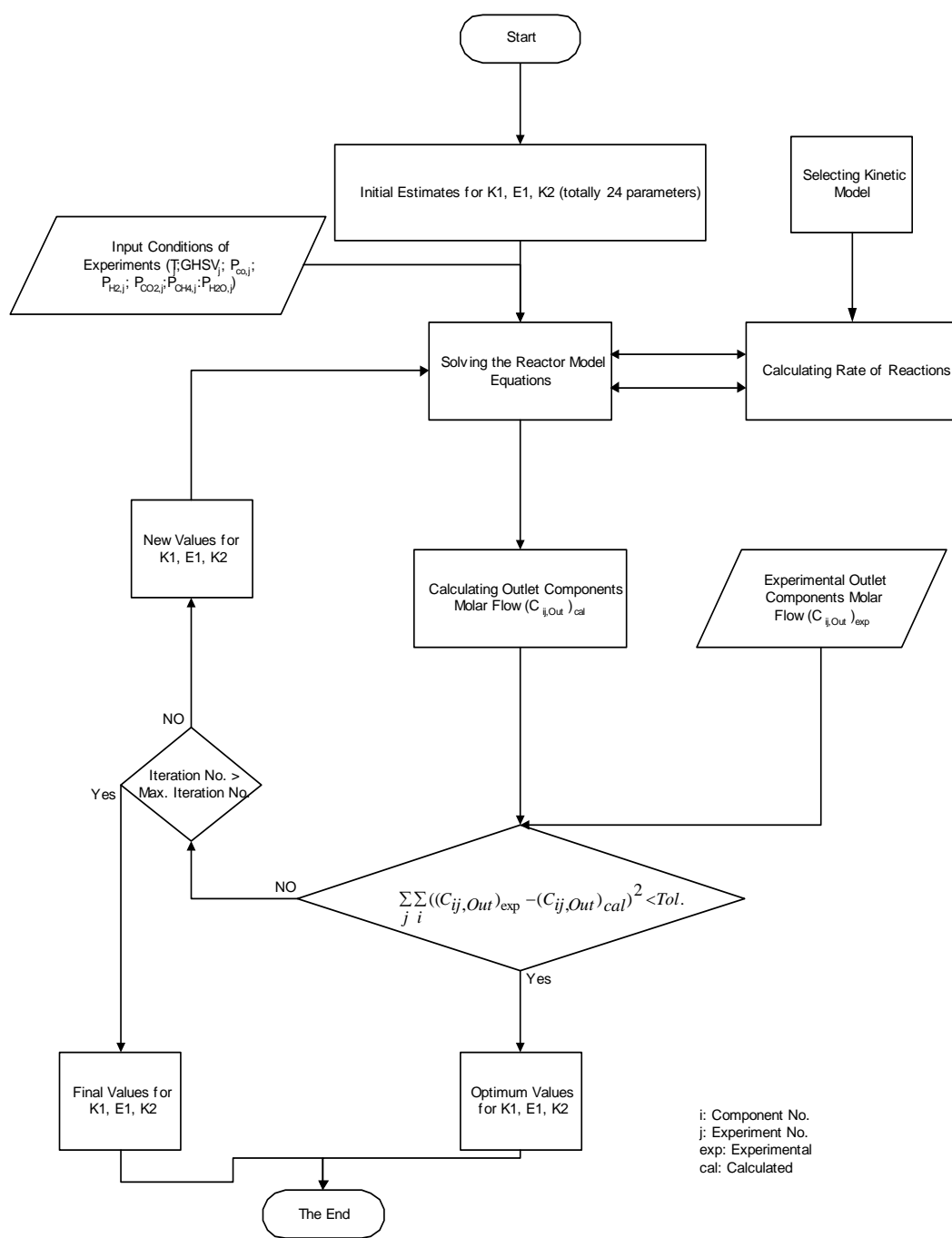


Fig. 5 The flow chart of the program for parameter estimation of the kinetic models.

The effectiveness factors are gathered in 35 points along the reactor for each simulation. Totally, 2520 series of data are being produced to be used for network training and validation. 1680 and 840 points were chosen respectively for network training and validation.

For training the networks, a variation of the back propagation algorithm is used: the Levenberg – Marquardt algorithm.

To find the suitable network, two different network structures are being tested. The networks consist of one input layer (13 neurons, 11 neurons for component mass fractions and two neurons for temperature and pressure); one or two hidden layer and one output layer (containing 8 neurons for component's effectiveness factors). The transfer functions of Sigmoid and Linear were chosen respectively for hidden and output layers. The two different Sigmoid transfer functions (tansig and logsig¹) has been applied for hidden layers. The training was carries on during 500 epochs, in each case.

At the end, different networks are compared. Training Mean Square Error (MSE) comparison shows that the best successful network found to learn the problem has two hidden layers with tansig transfer function and 9 and 8 neurons in the first and second hidden layers respectively.

TABLE IV GOAL FUNCTION FOR MODEL DISCRIMINATION

Kinetic model No.	Goal function (θ)	Kinetic model No.	Goal function (θ)
1	$5.8277 \cdot 10^{-09}$	14	$9.91363 \cdot 10^{-10}$
2	$5.9117 \cdot 10^{-09}$	15	$7.45533 \cdot 10^{-9}$
3	$5.7936 \cdot 10^{-09}$	16	$9.91363 \cdot 10^{-10}$
4	$5.9042 \cdot 10^{-09}$	17	$9.91363 \cdot 10^{-10}$
5	$7.4553 \cdot 10^{-09}$	18	$9.91363 \cdot 10^{-10}$
6	$5.5298 \cdot 10^{-09}$	19	$5.16151 \cdot 10^{-9}$
7	$5.4172 \cdot 10^{-09}$	20	-----
8	$5.8473 \cdot 10^{-09}$	21	$7.45533 \cdot 10^{-9}$
9	$7.4553 \cdot 10^{-09}$	22	-----
10	$6.3673 \cdot 10^{-09}$	23	$5.87014 \cdot 10^{-9}$
11	$6.5233 \cdot 10^{-09}$	24	$9.91363 \cdot 10^{-10}$
12	$5.2439 \cdot 10^{-09}$	25	$9.91363 \cdot 10^{-10}$
13	$7.4553 \cdot 10^{-09}$	26	$9.91363 \cdot 10^{-10}$

¹ Logsig (n)= $1/(1+\exp(-n))$; Tansig (n)= $2/(1+\exp(-2n))-1$

TABLE V KINETIC PARAMETERS DATA

$$(R_i \text{ (mol s}^{-1} \text{ kg cat}^{-1}) = K_i \exp(\frac{-E_i}{RT}) \frac{P_{H_2}^2}{P_{CO}})$$

Reaction No.	K_i (mol s ⁻¹ kgcat ⁻¹ kPa ⁻¹)	E_i (J mol ⁻¹)
1	$3.168 \cdot 10^{-5}$	738.78
2	$2.044 \cdot 10^{-2}$	15693
3	$6.255 \cdot 10^{-5}$	20.384
4	$3.423 \cdot 10^{-4}$	1.5607
5	$5.972 \cdot 10^{-6}$	164.06
6	$6.482 \cdot 10^{-6}$	86.934
7	$610.482 \cdot 10^{-6}$	81.753
8	$4.285 \cdot 10^{-3}$	5532.9

TABLE VI OPERATING CONDITIONS RANGE FOR PRODUCING TRAINING DATA

Parameter	Minimum	Maximum	No. of Points
Cooling Temperature (K)	530	570	4
Reactor Pressure (kPa)	1300	2100	3
Feed Molar Ratio of H ₂ / CO	0.7	1.5	6

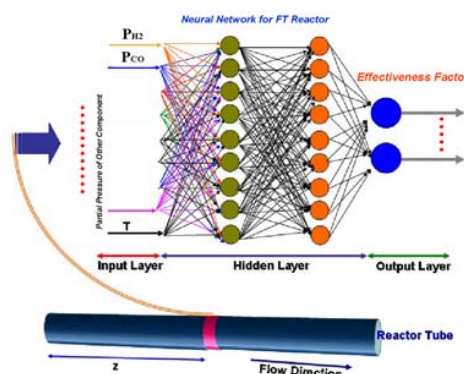


Fig 6. Effectiveness factors Neural network mechanism.

REFERENCES

- [1] Ketta J. J. Mc (1993). Encyclopedia of Chemical Processing and Design; Marcel Dekker; 3rd edition,
- [2] Raymond E. Kirk and Donald F. (1978). Othmer; Encyclopedia of chemical technology; John Wiley & Sons; 3rd edition
- [3] Parkinson G. (1997). Fischer – Tropsch Comes Back, Chemical Engineering, 39 – 40, 170
- [4] Hedden, K., Jess, A., Kuntze, T. (1994). From Natural gas to liquid hydrocarbons (1). A new concept for the production of liquid hydrocarbons from natural gas in remote areas; OIL GAS – European Magazine, 3, 42 – 44
- [5] Hedden, K., Jess, A., Kuntze, T. (1997). From Natural gas to liquid hydrocarbons (4). Production of diesel oil and wax by Fischer – Tropsch synthesis using a nitrogen rich synthesis gas investigation on a semi technical scale; Edröl Erdgas Kohle, 113, 12, 531-540,
- [6] Shiri Garakani A. R., Yeganeh Mehr J., Jafari Jozani Kh. (1998). Fischer – Tropsch reaction for production of gasoline on a coprecipitated iron catalyst modified with HZSM-5; 15th Canadian Symposium on Catalysis; 17 – 20 May; Quebec, Canada
- [7] Yegane Mehr J., Jafari Jozani Kh. (1998). FT synthesis catalyst production for producing liquid fuel from synthesis gas; Tahghigh, Quarterly Bulletin of RIPI, 28, 106 – 124
- [8] Shen W. J., Zhou J. L., Zhang B. J. (1994). Kinetics of Fischer – Tropsch synthesis over precipitated iron catalyst; Journal of natural gas chemistry; 4, 385 – 400
- [9] Zimmerman W.H. and Bukur D.B. (1990). Reaction kinetics over iron catalysts used for the fischer-tropsch synthesis; Canadian Journal of Chemical Engineering; 68, pp. 292-301.
- [10] Van der Laan G.P. and Beenackers A.A.C.M. (1999). Kinetics and Selectivity of the Fischer-Tropsch Synthesis: A Literature Review; Catalysis Reviews, 41, pp. 255-318
- [11] Nakhaei Pour A., Housaindokht M.R., Tayyari S.F., Zarkesh J., Alaei M.R. (2010); Kinetic studies of the Fischer-Tropsch synthesis over La, Mg and Ca promoted nano-structured iron catalyst; Journal of Natural Gas Science and Engineering, 2 (2-3), pp. 61-68.
- [12] TENG B., CHANG J., WAN H, LU J., ZHENG S., LIU Y., LIU Y., GUO X. (2007); A Corrected Comprehensive Kinetic Model of Fischer–Tropsch Synthesis; Chines Journal of Catalysis; 28 (8), PP. 687-695.
- [13] Ahmadi Marvast M., Sohrabi M., Zarrinpashne S., Baghmisheh Gh.; Chem. Eng. Technol.; 28(1), 78-86; 2005
- [14] José M. Serra, Avelino Corma, Antonio Chica, Estefania Argente, Vicente Botti; Can artificial neural networks help the experimentation in catalysis?; Catalysis Today; 81, 393–403; 2003
- [15] J. A. Conesa, J. A. Caballero, J. A. Reyes-Labarta; Artificial neural network for modeling thermal decompositions; J. Anal. Appl. Pyrolysis; 71, 343-352; 2004
- [16] E.J. Molga, B.A.A. van Woezik, K.R. Westerterp; Neural networks for modelling of chemical reaction systems with complex kinetics: oxidation of 2-octanol with nitric acid; Chemical Engineering and Processing; 39, 323–334; 2000
- [17] Daniel R. Parisi, Miguel A. Laborde; Modeling steady-state heterogeneous gas-solid reactors using feedforward neural networks; Computers and Chemical Engineering; 25, 1241-1250; 2001
- [18] Bub, G.; Baerns, M. (1980). Prediction of the performance of catalytic fixed bed reactors for Fischer – Tropsch synthesis; Chemical Engineering Science; 35, 348-355

Dr. Mahdi Ahmadi Marvast received his BSc in Chemical engineering in 1996 from Petroleum University in Abadan, Iran. He has received his MSc and PhD in Chemical Engineering from Amir kabir University of Technology in Tehran, Iran in 1998 and 2005 respectively. He has been working in the Research Institute of Petroleum Industry (RIPI) from 2000 and now is head of modelling and control department. He has published more than 40 papers in the journals and conferences in the past years.